Modeling and Prediction of Nonlinear Environmental System Using Bayesian Methods

Majdi Mansouri[a], Benjamin Dumont[b], Marie-France Destain[b]

[a] *Corresponding author, Université de Liége (GxABT) Département des Sciences et Technologies de l'Environnement, Gembloux, Belgium, Tel:+336 58 29 80 79, Fax: +333 25 71 76 47, E-mail: majdi.mansouri@utt.fr*
[b] *Université de Liége (GxABT) Département des Sciences et Technologies de l'Environnement, Gembloux, Belgium.*

Abstract

An environmental dynamic system is usually modeled as a nonlinear system described by a set of nonlinear ODEs. A central challenge in computational modeling of environmental systems is the determination of the model parameters. In these cases, estimating these variables or parameters from other easily obtained measurements can be extremely useful. This work addresses the problem of monitoring and modeling a leaf area index and soil moisture model (LSM) using state estimation. The performances of various conventional and state-of-the-art state estimation techniques are compared when they are utilized to achieve this objective. These techniques include the extended Kalman filter (EKF), particle filter (PF), and the more recently developed technique variational filter (VF). Specifically, two comparative studies are performed. In the first comparative study, the state variables (the leaf-area index LAI , the volumetric water content of the soil layer 1, HUR1 and the volumetric water content of the soil layer 2, HUR2) are estimated from noisy measurements of these variables, and the various estimation techniques are compared by computing the estimation root mean square error (RMSE) with respect to the noise-free data. In the second comparative study, the state variables as well as the model parameters are simultaneously estimated. In this case, in addition to comparing the performances of the various state estimation techniques, the effect of number of estimated model parameters on the accuracy and convergence of these techniques are also assessed. The results of both comparative studies show that the PF provides a higher accuracy than the EKF, which is due to the limited ability of the EKF to handle highly nonlinear processes. The results also show that the VF provides a significant improvement over the PF because, unlike the PF which depends on the choice of

sampling distribution used to estimate the posterior distribution, the VF yields an optimum choice of the sampling distribution, which also accounts for the observed data. The results of the second comparative study show that, for all techniques, estimating more model parameters affects the estimation accuracy as well as the convergence of the estimated states and parameters. However, the VF can still provide both convergence as well as accuracy related advantages over other estimation methods.

Keywords: State and Parameter estimation, variational filter, Particle filter, Extended Kalman filter, Nonlinear Environmental System, leaf area index and soil moisture model.

1. Introduction

Crop models such as EPIC [37], WOFOST [12], DAISY[17], STICS [9], and SALUS [7] are dynamic nonlinear models that describe the growth and development of a crop interacting with environmental factors (soil and climate) and agricultural practices (crop species, tillage type, fertilizer amount,). They are developed to predict crop yield and quality or to optimize the farming practices in order to satisfy environmental objectives, as the reduction of nitrogen lixiviation. More recently, crop models are used to simulate the effects of climate changes on the agricultural production. Nevertheless, the prediction errors of these models may be important due to uncertainties in the estimates of initial values of the states, in input data, in the parameters, and in the equations. The measurements needed to run the model are sometimes not numerous, whereas the field spatial variability and the climatic temporal fluctuations over the field may be high. The degree of accuracy is therefore difficult to estimate, apart from numerous repetitions of measurements.
For these reasons, the problem of state/parameter estimation represents a key issue in such nonlinear and non Gaussian crop models including a large number of parameters, while measurement noise exists in the data.

Several state estimation techniques are developed and used in practice. These techniques include the extended Kalman filter, particle filter, and more recently the variational filter. The classical Kalman Filter (KF) was developed in the 1960s [19], and is widely used in various engineering and science applications, including communications, control, machine learning, neuroscience, and many others. In the case where the model describing the system is assumed to be linear and Gaussian, the KF provides an optimal solution

[32, 15, 1, 26]. The KF has also been formulated in the context of Takagi-Sugeno fuzzy systems to handle nonlinear models, which can be described as a convex set of multiple linear models [10, 31, 28]. It is known that the KF is computationally efficient; however, it is limited by the non-universal linear and Gaussian modeling assumptions. To relax these assumptions, the extended Kalman filter [32, 15, 18, 24, 20] and the unscented Kalman filter [32, 15, 36, 27, 30] are developed. In extended Kalman filtering, the model describing the system is linearized at every time sample (in order to estimate the mean and covariance matrix of the state vector), and thus the model is assumed to be differentiable. Unfortunately, for highly nonlinear or complex models, the EKF does not usually provide a satisfactory performance. On the other hand, instead of linearizing the model to approximate the mean and covariance matrix of the state vector, the UKF uses the unscented transformation to improve the approximation of these moments. In the unscented transformation, a set of samples (called sigma points) are selected and propagated through the nonlinear model, which provides more accurate approximations of the mean and covariance matrix of the state vector, and thus more accurate state estimation.

Other state estimation techniques use a Bayesian framework to estimate the state and/or parameter vector [8]. The Bayesian framework relies on computing the probability distribution of the unobserved state given a sequence of the observed data in addition to a state evolution model. Consider an observed data set y, which is generated from a model defined by a set of unknown state variables and/or parameters z [8]. The beliefs about the data are completely expressed via the parametric probabilistic observation model, $P(y|z)$. The learning of uncertainty or randomness of a process is solved by constructing a distribution $P(z|y)$, called the posterior distribution, which quantifies our belief about the system after obtaining the measurements. According to Bayes rule, the posterior can be expressed as:

$$P(z|y) \propto P(y|z)P(z),$$

where $P(y|z)$ is the conditional distribution of the data given the vector, z, which is called the likelihood function, and $P(z)$ is the prior distribution, which quantifies our belief about z before obtaining the measurements. Thus, Bayes rule specifies how our prior belief, quantified by the priori distribution, is updated according to the measured data y. Unfortunately, for most nonlinear systems and non-Gaussian noise obser-

vations, closed-form analytic expressions of the posterior distribution of the state vector are untractable [21]. To overcome this drawback, a non-parametric Monte Carlo sampling based method called particle filtering [33, 14, 29] has recently gained popularity.

The Particle Filter approximates the posterior probability distribution by a set of weighted samples, called particles [3]. Since real-world problems usually involve high-dimensional random variables with complex uncertainty, the nonparametric and sample-based estimation of uncertainty (provided by the PF) has thus become quite popular to capture and represent the complex distribution $P(z|y)$ for nonlinear and non-Gaussian process models [3]. The PF has the ability to accommodate nonlinear and multi-modal dynamics, but at the cost of more computational complexity and storage requirements. Also, taking into account the stringent calculus and storage constraints, the propagation of a huge amount of particles has impeded the implementation of the PF in very challenging parameter estimation problems. As a consequence, the variational filter is proposed recently to enhance state estimation [25, 4] because VF yields an optimal choice of the sampling distribution by minimizing a Kullback-Leibler (KL) divergence criterion. In fact, variational calculus leads to a simple Gaussian sampling distribution whose parameters (which are estimated iteratively) also utilize the observed data, which provides more accurate and computationally efficient computation of the posterior distribution.

Each of the above state estimation techniques has its advantages and disadvantages. The VF can be applied to large parameter spaces, has better convergence properties, and is easier to implement than the PF, and both of them can provide improved accuracy over the EKF. The objective of this paper is to compare the performances of the EKF, PF, and VF when used to monitor and model a LSM process through the estimation of its state variables and model parameters. This comparative study is assess the accuracy and convergence of these techniques, as well as the effect of the size of the parameter space (i.e., number of estimated parameters) on the performances of these estimation techniques. Some practical challenges, however, can affect the accuracy of estimated states and/or parameters. Such challenges include the large number of states and parameters to be estimated, the presence of measurement noise in the data, and the availability of small number of measured data samples. The objective of this paper is two-fold: i) we study

the accuracy and convergence of EKF, UKF and PF techniques, ii) we investigate the effect of the above challenges on the performances of these techniques. Then, a comparative investigation are be conducted to study their performances under the same challenge mentioned above. The above analysis are be performed using an environment process model representing leaf area index and soil moisture (LSM) (i.e, the leaf-area index LAI, the volumetric water content of the layer 1, HUR1 and the volumetric water content of the layer 2, HUR2) and their abilities to estimate some of the key system parameters, which are needed to define the LSM model.

The rest of the paper is organized as follows. In Section 2, a statement of the problem addressed in this paper is presented, followed by descriptions of various commonly used state estimation techniques in Section 2.2. Then, in Section 3, the performances of the various state estimation techniques are compared through their application to estimate the state variables and model parameters of a LSM process. Finally, some concluding remarks are presented in Section 4.

2. Material and Methods

In this section, the mathematical formulation of the the state/parameter estimation problem is developed, according to the filtering approaches that are studied. In a second step, the dynamic model simulation is presented, and the problem is formulated.

2.1. Problem Statement

Here, the estimation problem of interest is formulated for a general system model. Let a nonlinear state space model be described as follows:

$$\begin{aligned} \dot{x} &= g(x, u, \theta, w), \\ y &= l(x, u, \theta, v), \end{aligned} \tag{1}$$

where $x \in \mathbb{R}^n$ is a vector of the state variables, $u \in \mathbb{R}^p$ is a vector of the input variables, $\theta \in \mathbb{R}^q$ is an unknown parameter vector, $y \in \mathbb{R}^m$ is a vector of the measured variables, $w \in \mathbb{R}^n$ and $v \in \mathbb{R}^m$ are process and measurement noise vectors, respectively, and g and l are nonlinear differentiable functions. Discretizing

the state space model (1), the discrete model can be written as follows:

$$\begin{aligned} x_k &= f(x_{k-1}, u_{k-1}, \theta_{k-1}, w_{k-1}), \\ y_k &= h(x_k, u_k, \theta_k, v_k), \end{aligned} \tag{2}$$

which describes the state variables at some time step (k) in terms of their values at a previous time step ($k-1$). Let the process and measurement noise vectors have the following properties: $\mathbf{E}[w_k] = 0$, $\mathbf{E}[w_k w_k^T] = \mathbf{Q}_k$, $\mathbf{E}[v_k] = 0$ and $\mathbf{E}[v_k v_k^T] = \mathbf{R}_k$. Since we are interested in estimating the state vector, x_k, as well as the parameter vector, θ_k, let's assume that the parameter vector is described by the following model:

$$\theta_k = \theta_{k-1} + \gamma_{k-1}. \tag{3}$$

which means that it corresponds to a stationary process, with an identity transition matrix, driven by white noise. In order to include the parameter vector θ_k into the state estimation problem, let's define a new state vector z_k that augments the state vector x_k and the parameter vector θ_k as follows:

$$z_k = \begin{bmatrix} x_k \\ \theta_k \end{bmatrix} = \begin{bmatrix} f(x_{k-1}, u_{k-1}, w_{k-1}, \theta_{k-1}) \\ \theta_{k-1} + \gamma_{k-1} \end{bmatrix}, \tag{4}$$

where $z_k \in \mathbb{R}^{n+q}$. Also, defining the augmented noise vector as:

$$\epsilon_{k-1} = \begin{bmatrix} w_{k-1} \\ \gamma_{k-1} \end{bmatrix}, \tag{5}$$

the model (2) can be written as,

$$z_k = \mathfrak{F}(z_{k-1}, u_{k-1}, \epsilon_{k-1}), \tag{6}$$

$$y_k = \mathfrak{R}(z_k, u_k, v_k), \tag{7}$$

where $\mathfrak{F}$ and $\mathfrak{R}$ are differentiable nonlinear functions. Thus, the objective here is to estimate the augmented state vector z_k, given the measurements vector y_k. Descriptions of some of the state estimation techniques that can be used to solve this estimation problem are presented next.

2.2. Description of State and Parameter Estimation Techniques

In this section, the formulations as well as the algorithms used in some of the state estimation techniques (EKF, PF and VF) are be presented.

2.2.1. extended Kalman filter

As the name indicates, EKF is an extension of the Kalman filter, where the model is linearized to estimate the covariance matrix of the state vector [22, 39]. As in KF, the state vector z_k is estimated by minimizing a weighted covariance matrix of the estimation error, i.e., $\mathbf{E}[(z_k - \widehat{z}_k)\mathbf{M}(z_k - \widehat{z}_k)^T]$, where $\mathbf{M}$ is a symmetric nonnegative definite weighting matrix. If all the states are equally important, $\mathbf{M}$ can be taken as the identity matrix, which reduces the covariance matrix to $\mathbf{P} = \mathbf{E}[(z_k - \widehat{z}_k)(z_k - \widehat{z}_k)^T]$. Such a minimization problem can be solved by minimizing the following objective function:

$$\mathbf{J} = \frac{1}{2} Tr\Big(\mathbf{E}[(z_k - \widehat{z}_k)(z_k - \widehat{z}_k)^T]\Big). \tag{8}$$

subject to the model defined in equations (6 and 7). To minimize the above objective function (8), EKF estimates the state vector using a two-step algorithm: prediction and estimation (or update), which are described next.

Prediction Step:

In the prediction step, one-step predictions of the augmented state vector and the measurement vector are calculated from the previously estimated state vector using the nonlinear model, i.e.,

$$\begin{aligned} \widehat{z}_{k|k-1} &= \mathfrak{F}(\widehat{z}_{k-1|k-1}, u_{k-1}), \\ \widehat{y}_{k|k-1} &= \mathfrak{R}(\widehat{z}_{k|k-1}, u_k). \end{aligned} \tag{9}$$

Estimation (Update) Step:

Then, an updated estimate of the augmented state vector is calculated after obtaining the measurement vector, y_k, as follows:

$$\begin{aligned} \mathbf{P}_{k|k-1} &= \mathbf{A}_{k-1}\mathbf{P}_{k-1|k-1} + \mathbf{G}_{k-1}\mathbf{Q}\mathbf{P}_{k-1}^T, \\ \mathbf{K}_k &= \mathbf{P}_{k|k-1}\mathbf{C}_k^T(\mathbf{C}_k\mathbf{P}_{k|k-1}\mathbf{C}_k^T + \mathbf{H}_k\mathbf{R}\mathbf{H}_k^T)^{-1}, \\ \mathbf{P}_{k|k} &= (I - \mathbf{K}_k\mathbf{C}_k)\mathbf{P}_{k|k-1}^T, \\ \widehat{z}_{k|k} &= \widehat{z}_{k|k-1} + \mathbf{K}_k(\widehat{y}_{k|k-1} - y_k), \end{aligned} \tag{10}$$

where $\mathbf{A}_{k-1} \approx \frac{\partial \mathfrak{F}}{\partial z}|_{\widehat{z}_{k-1|k-1}}$, $\mathbf{C}_{k-1} \approx \frac{\partial \mathfrak{R}}{\partial z}|_{\widehat{z}_{k-1|k-1}}$, $\mathbf{G}_{k-1} \approx \frac{\partial \mathfrak{F}}{\partial \epsilon}|_{\epsilon_{k-1}}$ and $\mathbf{H}_k \approx \frac{\partial \mathfrak{R}}{\partial v}|_{v_k}$ are the matrices of the linearized system model at every time step. And $\mathbf{Q}$ is the process noise covariance.

The EKF algorithm does not always provide a satisfactory performance, especially for highly nonlinear processes, because linearizing the process model does not necessarily provide good estimates of the mean of the state vector and the covariance matrix of the estimation error which are used in state estimation.

2.2.2. Particle Filter

A particle filter is an implementation of a recursive Bayesian estimator [16, 3]. Bayesian estimation relies on computing the posterior $p(z_k|y_{1:k})$, which is the density function of the unobserved state vector, z_k, given the sequence of the observed data $y_{1:k} \equiv \{y_1,\ y_2,\ \cdots,\ y_k\}$. However, instead of describing the required posterior distribution in a functional form, in this particle filter scheme, it is represented approximately as a set of random samples of the posterior distribution. These random samples, which are called the particles of the filter, are propagated and updated according to the dynamics and measurement models [13, 3]. The advantage of the PF is that it is not restricted by the linear and Gaussian assumptions, which makes it applicable in a wide range of applications. The basic form of the PF is also very simple, but may be computationally expensive. Thus, the advent of cheap, powerful computers over the last ten years is a key to the introduction and utilization of particle filters in various applications.

For a given dynamical system describing the evolution of the states and parameters that we wish to estimate, the estimation problem can be viewed as an optimal filtering problem [2], in which the posterior distribution, $p(z_k|y_{1:k})$, is recursively updated. Here, the dynamical system is characterized by a Markov state evolution model, $p(z_k|z_{1:k-1}) = p(z_k|z_{k-1})$, and an observation model, $p(y_k|z_k)$. In a Bayesian context, the task of state estimation can be formulated as recursively calculating the predictive distribution $p(z_k|y_{1:k-1})$ and the filtering distribution $p(z_k|y_{1:k})$ as follows,

$$p(z_k|y_{1:k-1}) = \int_{\mathbb{R}^n} p(z_k|z_{k-1})p(z_{k-1}|y_{1:k-1})dz_{k-1},$$
$$\text{and} \quad p(z_k|y_{1:k}) = \frac{p(y_k|z_k)p(z_k|y_{1:k-1})}{p(y_k|y_{1:k-1})},$$
$$\text{where} \quad p(y_k|y_{1:k-1}) = \int_{\mathbb{R}^x} p(y_k|z_k)p(z_k|y_{1:k-1})dz_k. \tag{11}$$

The state vector z_k is assumed to follow a Gaussian model, $z_k \sim \mathcal{N}(\mu_k, \lambda_k)$, where at any time instant k, the expectation μ_k and the covariance matrix λ_k are both constants. Thus, the marginal state distribution is obtained by integrating over the mean and covariance matrix as follows,

$$p(z_k|z_{k-1}) = \int \mathcal{N}(z_k|\mu_k, \lambda_k)p(\mu_k, \lambda_k|z_{k-1})d\mu_k d\lambda_k, \tag{12}$$

where the integration with respect to the covariance matrix leads to the known class of scale mixture distributions introduced by Barndorff-Nielsen [6] for the scalar case.

The nonlinear nature of the system model leads to intractable integrals when evaluating the marginal state distribution, $p(z_k|z_{k-1})$. Therefore, Monte Carlo approximation is utilized, where the joint posterior distribution, $p(z_{0:k}|y_{1:k})$, is approximated by the point-mass distribution of a set of weighted samples (particles) $\{z_{0:k}^{(i)}, \ell_k^{(i)}\}_{i=1}^N$, i.e.,:

$$\hat{p}_N(z_{0:k}|y_{1:k}) = \sum_{i=1}^{N} \ell_k^{(i)} \delta_{z_{0:k}^{(i)}}(d\, z_{0:k}) / \sum_{i=1}^{N} \ell_k^{(i)}, \tag{13}$$

where $\delta_{z_{0:k}^{(i)}}(d\, z_{0:k})$ denotes the Dirac function, and N is the total number of particles. Based on the same set of particles, the marginal posterior probability of interest, $p(z_k|y_{1:k})$, can also be approximated as follows:

$$\hat{p}_N(z_k|y_{1:k}) = \sum_{i=1}^{N} \ell_k^{(i)} \delta_{z_k^{(i)}}(d\, z_k) / \sum_{i=1}^{N} \ell_k^{(i)}. \tag{14}$$

In the Bayesian importance sampling (IS) method, the particles $\{z_{0:k}^{(i)}\}_{i=1}^N$ are sampled according to a distribution,

$$\pi(z_{0:k}|y_{1:k}) = p(z_k|z_{k-1}) = \int \mathcal{N}(z_k|\mu_k, \lambda_k)p(\mu_k, \lambda_k|z_{k-1})d\mu_k d\lambda_k, \tag{15}$$

Then, the estimate of the augmented state $\widehat{z}_k$ can be approximated by a Monte Carlo scheme:

$$\widehat{z}_k = \sum_{i=1}^{N} \ell_k^{(i)} z_k^{(i)}, \tag{16}$$

where $\ell_k^{(i)}$ are the corresponding importance weights:

$$\ell_k^{(i)} \propto \frac{p(y_{1:k}|z_{0:k}^{(i)})p(z_{0:k}^{(i)})}{\pi(z_{0:k}^{(i)}|y_{1:k})}. \tag{17}$$

A common problem with the sequential importance sampling particle filter is the degeneracy phenomenon, where after a few iterations, all but one particle have negligible weights. It is shown [38] that the variance of the importance weights can only increase over time, and thus, it is impossible to avoid the degeneracy phenomenon. This degeneracy implies that a large computational effort is devoted to updating particles whose contribution to the approximation of $p(z_k|y_{0:k})$ is almost zero. A suitable measure of degeneracy of the algorithm is the effective sample size N_{eff} introduced in [16] and [23] and defined as,

$$N_{eff} = \frac{1}{\sum_{i=1}^{N}(\ell_k^{(i)})^2} \tag{18}$$

where $\ell_k^{(i)}$ is the normalized weight obtained using (17).

In summary, particle filtering suffers from two major drawbacks. First, its efficient implementation requires the ability to sample from $p(z_k|z_{k-1})$, which does not take into account current the observed data, y_k, and thus many particles can be wasted in low likelihood (sparse) areas.The second drawback is that propagating such a huge amount of particles and their corresponding weights increases the computational complexity. These issues are addressed by the variational filter, which is described in the next section. The PF algorithm for state/parameter estimation is summarized in Algorithm 1.

2.2.3. variational filter

The variational filter was developed [25, 4] to address the limitations encountered in particle filtering. Unlike the PF algorithm, the temporal dependence in the VF is reduced to a single Gaussian statistic instead of a huge number of particles. This helps dramatically reduce the computational complexity associated with state estimation, especially since the computation time grows proportionally with the number of particles. Also, the estimation accuracy achieved in particle filtering depends on the choice of the importance sampling

Algorithm 1: Particle Filtering algorithm

Input: y_k, μ_0, λ_0

Output: $\widehat{z}_k$

for $i = 1, 2, \ldots$ **do**

Importance sampling step:

Sample $\widetilde{z}_k^{(i)} \sim \pi(z_k^{(i)} | z_{0:k-1}^{(i)}, y_{1:k})$, according the equation (12), and set $\widetilde{z}_{0:k}^{(i)} = (z_{0:k-1}^{(i)}, z_k^{(i)})$;

Compute the approximated joint distribution, $\hat{p}_N(z_{0:k}|y_{1:k})$, using equation 13;

Evaluate importance weights using equation (17);

Normalize importance weights:

$$\widetilde{\ell}_k^{(i)} = \frac{\ell_k^{(i)}}{\sum_{j=1}^{N} (\ell_k^{(j)})}$$

Selection step:

if $N_{eff} = \frac{1}{\sum_{i=1}^{N} (\ell_k^{(i)})^2} < N_{threshold}$ **then**

Resample with replacement N particles $\{z_{0:k}^{(i)}\}_{i=1}^{N}$ from the set $\{\widetilde{z}_{0:k}^{(i)}\}_{i=1}^{N}$ according to the normalised importance weights, $\ell_k^{(i)} = \widetilde{\ell}_k^{(i)}$;

Compute the estimated state using equation (16);

end

end

Return the augmented state estimation $\widehat{z}_k$.

distribution. The VF, however, yields an optimal choice of the sampling distribution over the state variable by minimizing the Kullback-Leibler (KL) divergence. In fact, variational calculus leads to a simple Gaussian sampling distribution, $p(z_k|z_{k-1}, y_k)$ whose parameters (which are estimated iteratively) also utilize the observed data, y_k.

In Bayesian estimation, the distribution of interest for state estimation takes the form of a marginal posterior distribution $p(z_k|y_{1:k})$. The VF approximates the posterior distribution, $p(z_k|y_{1:k})$, by a separable distribution $q(z_k) = \prod_i q(z_k^i)$ that minimizes the following KL divergence criterion:

$$
\begin{aligned}
D_{\mathrm{KL}}(q||p) &= \int q(z_k) \log \frac{q(z_k)}{p(z_k|y_{1:k})} dz_k, \\
\text{where} \quad q(z_k) &= \prod_i q(z_k^i)
\end{aligned} \tag{19}
$$

subject to the constraint $\int q(z_k)dz_k = \prod_i \int q(z_k^i)dz_k^i = 1$. The above KL divergence criterion can be minimized using the Lagrange multiplier method, which yields the following separable approximate distribution [35, 8, 11],

$$
q(z_k^i) \propto \exp\langle \log\, p(y_{1:k}, z_k)\rangle_{\prod_{j\neq i} q(z_k^j)}, \tag{20}
$$

where $\langle\cdot\rangle_{q(z_k^j)}$ denotes the expectation operator relative to the distribution $q(z_k^j)$. Therefore, these dependent parameters can be jointly and iteratively updated. Taking into account the separable approximate distribution $q(z_{k-1})$ at time $k-1$, the filtering distribution $p(z_k|y_{1:k})$ is sequentially approximated according to the following scheme:

$$
\hat{p}(z_k|y_{1:k}) \quad \propto \quad p(y_k|z_k)p(z_k). \tag{21}
$$

Therefore, through a simple integral with respect to μ_{k-1}, the filtering distribution $p(z_k|y_{1:k})$ can be sequentially updated. However, the state vector z_k does not have a tractable approximate distribution because of the nonlinear nature of the system model. By combining equations (20) and (21), we have,

$$
q(z_k) \propto p(y_k|z_k)\mathcal{N}(\langle\mu_k\rangle, \langle\lambda_k\rangle). \tag{22}
$$

which suggests an importance sampling (IS) procedure to approximate the posterior, where samples are drawn from the Gaussian distribution $\mathcal{N}(\langle\mu_k\rangle, \langle\lambda_k\rangle)$ and weighted according to their likelihoods:

$$
z_k^{(i)} \sim \mathcal{N}(\langle\mu_k\rangle, \langle\lambda_k\rangle),\ \ell_k^{(i)} \propto \prod_{j=1}^{N} p(z_k^j|z_k^{(i)}). \tag{23}
$$

Then, the estimated state, $\widehat{z}_k$, can be approximated by the following Monte Carlo scheme:

$$
\widehat{z}_k = \sum_{i=1}^{N} \ell_k^{(i)} z_k^{(i)}. \tag{24}
$$

In a Bayesian inference framework, besides updating the filtering distribution $p(z_k|y_{1:k})$, the predictive distribution $p(z_k|y_{1:k-1})$ needs to be computed. The predictive distribution $p(z_k|y_{1:k-1})$ can be efficiently

updated by variational inference. Taking into account the separable approximate distribution $q(z_{k-1}) \propto p(z_{k-1}|y_{1:k-1})$, the predictive distribution can be expressed as,

$$p(z_k|y_{1:k-1}) \quad \propto \quad \int p(z_k|z_{k-1})q(z_{k-1})dz_{k-1}.$$

Similar to the filtering distribution, the predictive distribution that minimizes the Kullback-Leibler divergence yields the following Gaussian distribution:

$$q_{k|k-1}(z_k) \quad \propto \quad \mathcal{N}(\langle \mu_k \rangle_{q_{k|k-1}}, \langle \lambda_k \rangle_{q_{k|k-1}}), \tag{25}$$

and the predictive expectations of the state can be evaluated by the following expressions:

$$\begin{aligned} \langle z_k \rangle_{q_{k|k-1}} &= \langle \mu_k \rangle_{q_{k|k-1}}, \\ \langle z_k z_k^T \rangle_{q_{k|k-1}} &= \langle \lambda_k \rangle_{q_{k|k-1}}^{-1} + \langle \mu_k \rangle_{q_{k|k-1}} \langle \mu_k \rangle_{q_{k|k-1}}^T. \end{aligned} \tag{26}$$

Compared with the PF, the computational cost and the memory requirements associated with the VF are dramatically reduced by the variational approximation in the prediction phase. In fact, the expectations involved in the computation of the predictive distribution have closed forms, avoiding the use of Monte Carlo integration. The VF algorithm for state/parameter estimation is summarized in Algorithm 2.

In the next Section, these state estimation techniques (EKF, PF, and VF) are used to estimate the states variables (the leaf-area index LAI , the volumetric water content of the layer 1, HUR1 and the volumetric water content of the layer 2, HUR2) as well as the model parameters of a LSM process.

Algorithm 2: variational filtering algorithm

Input: y_k, μ_0, λ_0

Output: $\widehat{z}_k$

for $i = 1, 2, \ldots$ **do**

Predict $p(z_k|y_{1:k-1})$ according to the equation (25);

The predicted expectation $\langle z \rangle_{q_{k|k-1}}$ is calculated using equation (26);

Generate N samples $\{z_k^{(i)}, \ell_k^{(i)}\}_{k=1}^N$ from $q(z_k)$, where $q(z_k) \propto p(y_k|z_k)\mathcal{N}(\langle \mu_k \rangle, \langle \lambda_k \rangle)$ using equation (23);

if $N_{eff} = \frac{1}{\sum_{i=1}^N (\ell_k^{(i)})^2} < N_{threshold}$ **then**

Resample with replacement N particles $\{z_{0:k}^{(i)}\}_{i=1}^N$ from the set $\{\widetilde{z}_{0:k}^{(i)}\}_{i=1}^N$ according to the normalised importance weights, $\ell_k^{(i)} = \widetilde{\ell}_k^{(i)}$;

Compute the estimated state using equation (24):

$$\widehat{z}_k = \sum_{i=1}^{N} \ell_k^{(i)} z_k^{(i)}$$

end

end

Return the augmented state estimation $\widehat{z}_k$.

3. Simulation Results Analysis

Next, the Crop model, that are be used in our analysis, are be described.

3.1. Crop model

The original data were issued from experiments carried out on a silty soil in Belgium, with a wheat crop (*Triticum aestivum* L., cultivar Julius), during 3 consecutive years, the crop seasons 2008-09, 2009-10 and 2010-11. The measurements were the results of 4 repetitions by date, each one of them being performed on a small block (2m times 6m) randomly spread over the field to ensure the measurements independence. A wireless monitoring system (eKo pro series system, Crossbow) completed by a micrometeorological station

was used for measuring continuously soil and climate characteristics. Especially, the measurements of soil water content were performed at 20 and 50 cm depth.

The plant characteristics (LAI and biomass) were also measured using reference techniques at regular intervals (2 weeks) along the crop seasons. The reference measurements were each year performed since the middle of February (around Julian day 410) till harvest. During the season 2008-2009, yields were quite high and close to the optimum of the cultivar. This is mainly explained by the good weather conditions and a sufficient nitrogen nutrition level. The season 2009-2010 and 2010-11 were known to induce deep water stresses, and thus characterized by yield losses. In 2009-10 they occurred at early spring and early June, but stayed limited. The following year, deeper water stresses occurred from February till beginning of June. In the summer, rainfall came back and allowed good grain yield while low straws yield were never compensated.

The model for which the methods are tested is Mini-STICS model. The model equations are presented in Appendix A [34], and the model parameters presented at Table 1. The dynamic equations indicates how each state variable evolves from one day to the next as a function of the current values of the state variables, of the explanatory variables, and of the parameters value. Encoding these equations over time allows one to eliminate the intermediate values of the state variables and relate the state variables at any time to the explanatory variables on each day. The model structure can be derived from the basic conservation laws, namely material and energy balances.

In the first step we are be interested to compare the estimation performances of EKF, PF and VF in estimating three state variables of the mini-STICS model : the leaf-area index LAI , the volumetric water content of the layer 1, HUR1 and the volumetric water content of the layer 2, HUR2. Based on the model equations described in Appendix A, the mathematical model of the LAI and soil moisture (called in the rest of the document LSM model) is given by:

$$\begin{cases} LAI(t) = f_1(LAI(t-1), \theta) \\ HUR1(t) = f_2(HUR1(t-1), \theta) \\ HUR2(t) = f_3(HUR2(t-1), \theta) \end{cases} \tag{27}$$

where t is the time step (one day), f_{1-3} are the corresponding model function, and θ is the vector of parameters driving the simulations (Table 1).

Here, we therefore assume that some of the states are wrong simulated by the model, and our objective is to re-estimate them, under the hypothesis that the states are measured at some moment, along the season. Discretizing the model (27) using a sampling interval of Δt, it can be written as:

$$\begin{cases} LAI_k = \Big[g_1(\theta)\Big]\Delta t + LAI_{k-1} + w_k^1 \\ HUR1_k = \Big[g_2(\theta)\Big]\Delta t + HUR1_{k-1} + w_k^2 \\ HUR2_k = \Big[g_3(\theta)\Big]\Delta t + HUR2_{k-1} + w_k^3 \end{cases} \tag{28}$$

where, $w^j{}_{,j\in\{1,..,3\}}$ is a measurement Gaussian noise with zero mean and known variance $\sigma^2_{w^j}$.

3.2. Generation of Dynamic Data

To go further in the research, it appear now to own data on which running the model. Indeed, the results may depend on the details of the model, on the way/quality the data are generated/measured with and on the specific data that are used. To be independent of these consideration, we are generate dynamic data from the LSM. The model is first used to simulate the responses LAI_k , $HUR1_k$, $HUR2_k$ as functions of time of the first recorded climatic variable of the crop season 2008-2009. These simulated states, which are assumed to be noise free, are then contaminated with zero mean Gaussian errors, i.e., a measurement noise $v_{k-1} \sim \mathcal{N}(0, \sigma_v^2)$.

Considering a value of $\sigma_v^2 = 0.1$ the following data set can be generated. Figure 1 shows the changes in the three state variables. The sampling time used for discretization is 1 day and the LSM model parameters as well as other physical properties are shown in Table 1. The parameter values are determined in [5].

3.3. Comparative Study 1: Estimation of State Variables from Noisy Measurements

At this point of the research, the model parameters are assumed to be constants, and at their true value presented in Table 1. Therefore, we consider the state vector that we wish to estimate as:

$$z_k = x_k = [LAI_k \; HUR1_k \; HUR2_k]^T,$$

Eventually, to perform comparison between the techniques, the estimation root mean square errors (RMSE) criteria are be used and calculated on the states (with respect to the noise free data)

$$\text{RMSE} = \sqrt{E\left((\mathbf{x} - \widehat{\mathbf{x}})^2\right)} \tag{29}$$

Where $\mathbf{x}$ (resp. $\widehat{\mathbf{x}}$) is the true parameter/state (resp. the estimated parameter/state).

The simulation results of estimating the three states: the leaf-area index LAI_k, $HUR1_k$ the volumetric water content of the layer 1 and $HUR2_k$ the volumetric water content of the layer 2 using EKF, PF and VF are shown in Figures 2(a,b,c), Figures 2(d,e,f) and Figures 2(g,h,i), respectively. Also, the estimation root mean square errors (RMSE) for the estimated states are shown in Table 2. It can be observed from Figure 2 and Table 2 that EKF resulted in the worst performance of all estimation techniques, which is expected due to the limited ability of EKF to accurately estimate the mean and covariance matrix of the estimated states through lineralization of the nonlinear process model. The results also show that the VF provides a significant improvement over the PF, which is due to the fact that the VF yields an optimal choice of the sampling distribution, $p(z_k|z_{k-1}, y_k)$, by minimizing a KL divergence criterion that also utilizes the observed data y_k.

3.4. Comparative Study 2: Simultaneous Estimation of State Variables and Model Parameters

The model (28) assumes that the parameters are fixed and/or are determined previously. However, the model involves several parameters that are usually not exactly known, or that have to be estimated. Estimating these parameters, to completely define the model, usually requires several experiment setups, which can be expensive and challenging in practice. In a second step, in this work, we propose to use a Bayesian approach that can considerably simplify the task of modeling compared to the conventional experimentally intensive methods. Let's thus consider that some of the parameter have to be estimated to improve the simulations, by example the $ADENS$, $DLAIMAX$ and $PSISTURG$ parameter. $ADEN$S is the parameter of compensation between stem number and plant density, $DLAIMAX$ is the maximum rate of the setting up of LAI and $PSISTURG$ is the absolute value of the potential of the beginning of decrease

in the cellular extension. To estimate these parameters, the following equations that describe their evolution are also needed:

$$\begin{cases} ADENS_k = ADENS_{k-1} + \gamma_k^1 \\ DLAIMAX_k = DLAIMAX_{k-1} + \gamma_k^2 \\ PSISTURG_k = PSISTURG_{k-1} + \gamma_k^3 \end{cases} \tag{30}$$

where, $\gamma^j{}_{,j\in\{1,..,3\}}$ is a process Gaussian noise with zero mean and known variance $\sigma^2_{\gamma^j}$.

The model (28) needs to incorporate the evolution of these parameters as follows:

$$\begin{cases} LAI_k = \Big[g_1(\theta_{k-1})\Big]\Delta t + LAI_{k-1} + w_k^1 \\ HUR1_k = \Big[g_2(\theta_{k-1})\Big]\Delta t + HUR1_{k-1} + w_k^2 \\ HUR2_k = \Big[g_3(\theta_{k-1})\Big]\Delta t + HUR2_{k-1} + w_k^3 \end{cases} \tag{31}$$

Where, g is nonlinear differentiable function, it can be used to compute the predicted state from the previous estimate.

Hence, the discrete nonlinear system model of the LAI and soil moisture can be written as:

$$\begin{cases} f1 : LAI_k = \Big[g_1(\theta_{k-1})\Big]\Delta t + LAI_{k-1} + w_k^1 \\ f2 : HUR1_k = \Big[g_2(\theta_{k-1})\Big]\Delta t + HUR1_{k-1} + w_k^2 \\ f3 : HUR2_k = \Big[g_3(\theta_{k-1})\Big]\Delta t + HUR2_{k-1} + w_k^3 \\ f4 : ADENS_k = ADENS_{k-1} + \gamma_k^1 \\ f5 : DLAIMAX_k = DLAIMAX_{k-1} + \gamma_k^2 \\ f6 : PSISTURG_k = PSISTURG_{k-1} + \gamma_k^3 \end{cases} \tag{32}$$

where, $f_k{}_{,k\in\{1,...,6\}}$ are some nonlinear functions, it is desired to estimate the parameter vector θ given dynamic measurements of the state variables LAI, $HUR1$ and $HUR2$.

In the following, we denote $w = (w_1 \;\; w_2 \;\; w_3)^T$, and $\gamma = (\gamma^1 \;\; \gamma^2 \;\; \gamma^3)^T$, respectively the measurement and process noise vectors, which quantify (i) errors in the measurements and (ii) randomness in the process.

Note that we are forming the augmented state:

$z_k = [x_k \;\; \theta_k]^T = [LAI_k \;\; HUR1_k \;\; HUR2_k \;\;\; ADENS_k \;\; DLAIMAX_k \;\; PSISTURG_k]^T$

as a 6 by 1 matrix with the following:

$$\begin{cases} x_k(1,:) & -> & LAI_k \\ x_k(2,:) & -> & HUR1_k \\ x_k(3,:) & -> & HUR2_k \\ \theta_k(1,:) & -> & ADENS_k \\ \theta_k(2,:) & -> & DLAIMAX_k \\ \theta_k(3,:) & -> & PSISTURG_k \end{cases} \tag{33}$$

The idea here is that, if a dynamic model structure is available, the model parameters can be estimated using one of state estimation technique. State estimation is a system-engineering approach, in which the states (and sometimes the parameters) of a state space model can be estimated given time-series dynamic measurements of some of the state variables.

Several state estimation techniques are developed, which can be used to solve this nonlinear state estimation problem, and include Extended Kalman Filtering, Particle Filtering, Variational Filtering, and others. In this work, the EKF, PF and VF are be used to illustrate the idea of modeling LAI and soil moisture.

In this section, we are interested in examining the effect of the number of estimated parameters on the estimation performances of EKF, PF and VF and in estimating the states and parameters of the LSM process model, during the first crop season 2008-2009 (unstressed growth data).

To investigate the effect of the number of estimated model parameters on the performances of the different state estimators, this comparative study are be conducted through the following three cases, which are summarized below. In all cases, it is assumed that three states (LAI_k, $HUR1_k$ and $HUR2_k$) are measured.

1. Case 1: the three states (LAI, $HUR1$ and $HUR2$) along with the parameter $ADENS$ are be estimated.
2. Case 2: the three states (LAI, $HUR1$ and $HUR2$) and two parameters ($ADENS$ and $DLAIMAX$) are be estimated.

3. Case 3: the three states (LAI, $HUR1$ and $HUR2$) and three parameters ($ADENS$, $DLAIMAX$ and $PSISTURG$) are be estimated.

The state and parameter estimation results for the three cases using EKF are shown in Figures 3 to 5; similarly, Figures 6 to 8 show the simulation results using PF, and Figures 9 to 11 show the simulation results using VF.

Moreover, Table 3 compares the estimation performances of EKF, PF and VF for case 1 in terms of the estimation root mean square errors (RMSE) for the three states LAI, $HUR1$ and $HUR2$ (with respect to the noise free data) and the mean of the estimated parameter $DLAIMAX$ at steady state. Tables 4 and 5 provide similar comparisons for cases 2 and 3, respectively, (i.e., estimating the three states and the parameters $ADENS$ and $DLAIMAX$ in case 2, and estimating the three states and the parameters $ADENS$, $DLAIMAX$, and $PSISTURG$ in case 3).

Comparing the estimation performances of EKF, PF and VF based on the simulation results shown in Tables 4 and 5, it is observed, as expected, that the root mean square errors (RMSE) of estimated states increase for all estimation techniques as the number of estimated states and parameters increases. Also, VF shows improved estimation performance over EKF and PF (and PF showed improved estimation performance over EKF) in estimating the states and parameters in all cases. In particular, the EKF is able to estimate the three states and one parameter, $DLAIMAX$, as shown in Figure 3.

However, when EKF is used in case 2 (case 3) to estimate the three states and respectively two or three parameters, the estimates of $PSISTURG$ and $DLAIMAX$ did not converge to the true values using the available data. The PF is able to estimate the three states and one (two) parameter(s), $ADENS$ ($ADENS$ and $DLAIMAX$), as shown in Figure 5 (Figure 6). However, when PF is used in case 3 to estimate the three states and all three parameters ($ADENS$, $DLAIMAX$ and $PSISTURG$), the estimate of $PSISTURG$ did not converge to the true value using the available data. The VF is able to estimate the three states and the parameters in all cases. However, the RMSE of the estimated states (with respect to the noise free data) using PF is less than the RMSE obtained using EKF, but it is higher than the RMSE obtained using the VF. Also, using PF, the parameter estimates show improved convergence rates to their true values over

the EKF, but worse convergence rates compared to the VF. Hence, as the number of states and parameters to be estimated increases, the VF shows improved estimation performance over the EKF and PF.

3.5. The Effect of driving variables

We applied the different algorithms described above; EKF, PF and VF to simulate the responses of the leaf-area index LAI_k, the volumetric water content of the layer 1 $HUR1_k$ and the volumetric water content of the layer 2 $HUR2_k$ as functions of time; in the second crop season 2009-2010 (season with deep water stresses). And respectively the above techniques are used for estimating the three model parameters; $ADENS$, $DLAIMAX$ and $PSISTURG$. From figure 13 (resp. Tables 6 to 8), we can show that variational filtering algorithm outperforms the classical algorithms, and demonstrate the performance and the good behavior of the proposed algorithm when the growing season is varied.

Here, we assume that a Gaussian noise is added to the time profiles of the metabolites. In order to show the performance of the states estimation techniques in the presence of measurement noise, five different measurements noise values, 0.1, 0.15, 0.2, 0.25 and 0.3, are considered. The RMSEs using the three techniques are summarized in Table 9. The simulation results of estimating the three states; leaf-area index LAI_k, the volumetric water content of the layer 1 $HUR1_k$ and the volumetric water content of the layer 2 $HUR2_k$ using EKF, UKF and PF when the variances noise vary in $\{0.1, 0.3\}$.

In other words, for the three estimation techniques, the estimation RMSE of the three states LAI_k, $HUR1_k$ and $HUR2_k$ increases from the first comparative study (noise variance = 0.1) to case (where the noise variance = 0.3). For example, the RMSEs obtained using EKF for LAI where the noise variance = 0.1 and = 0.2 are 0.0634, and 0.0639, respectively, which increase as the noise variance increases (refer to Table 9). This observation is valid for the other state variables LAI_k, $HUR1_k$ and $HUR2_k$.

4. Conclusions

In this paper, state estimation techniques are used to predict simultaneously three state variables (Leaf area index (LAI) and soil moisture model for a winter wheat crop) and several parameters. Various state estimation techniques, which include the extended Kalman filter, particle filter, and variational filter, are

compared as they are used to achieve this objective. Two comparative studies are conducted to compare the estimation performances of these three estimation techniques. In the first comparative study, EKF, PF and VF are used to estimate the three state variables (Leaf area index (LAI) and the moisture content of the two top soil layers) of the LSM process. In this second comparative study, the state variables are model parameters are simultaneously estimated, and the effect of number of estimated parameters on the performances of the three estimation techniques is investigated. The simulation results of both comparative studies show that the PF provides a higher accuracy than the EKF due to the limited ability of the EKF to deal with highly nonlinear process models. The results also show that the VF provides a significant improvement over the PF. This is because, unlike the PF which depends on the choice of sampling distribution used to estimate the posterior distribution, the VF yields an optimum choice of the sampling distribution, which also utilizes the observed data. The results of the second comparative study show that, for all techniques, estimating more model parameters affects the estimation accuracy as well as the convergence of the estimated states and parameters. The VF, however, still provides advantages over other methods with respect to estimation accuracy as well convergence.

5. Appendix A

Leaf Area Index

$$DELTAI(J) = LAI(J) - LAI(J-1) = \frac{DLAIMAX}{[1 - \exp(5.5 \times (2.2 - ULAI(J)))]} \times (TCULT(J-1) - TCMIN) \times TURFAC(J) \times EFDENSITE \times DENSITE$$

$$ULAI(J) = 2.2 + (3 - 2.2) \times \frac{SUDEVCULT(J)}{NBDJ_{AMF-LAX}}$$

$$EFDENSITE = (\frac{DENSITE}{BDENS})^{ADENS}$$

Soil Water Evaporation

$$EOS(J) = ETP(J) \times \exp(EXTIN - 0.2) \times LAI(J)$$

$$HA = \frac{ARGI}{100} \times \frac{DA_1}{15}$$

$$HI = \frac{HUCC_1}{10}$$

$$A = 0.5 \times ACLIM \times (0.63 - HA)^{53} \times (HI - HA)$$

$$\sum ES(J) = \sqrt{(2 \times A \times \sum EOS(J) + A^2)} - A$$

$$\sum EOS(J) = \begin{cases} \sum EOS(J-1) + EOS(J) \\ EOS(J) \end{cases}$$

$$\begin{cases} \text{if} \quad \sum ES(J-1) \quad > \quad PLUIE(J) \\ \text{else} \end{cases}$$

$$\sum ES(J) = \begin{cases} \sum ES(J-1) + ES(J-1) \\ ES(J) \end{cases}$$

$$\begin{cases} \text{if} \quad \sum ES(J-1) \quad > \quad PLUIE(J) \\ \text{else} \end{cases}$$

$$ES_1(J) = \min(HUR1(J-1) - 10 \times HA \times EPAIS1, ES(J))$$

$$HUR1(J) = HUR1(J-1) - \frac{ES_1(J)}{EPAIS1}.$$

318 **Transpiration**

$$EO(J) = \frac{ETP(J) \times (1 + (KMAX - 1)}{(1 + \exp(-1.5 \times (LAI(J) - 3)))}$$

$$EOP(J) = \frac{(EO(J) - EOS(J))(1.4 - 0.4 \times (ES(J)))}{EOS(J)}$$

$$S = -\frac{4.6}{ZLABOUR - ZPENTE}$$

$$ZDEMI(J) = \max(ZRAC(J) - ZPRLIM + ZPENTE, \frac{1.4}{S})$$

$$LRAC_1(J) = \frac{LVOPT}{(1 + \exp(-S \times (PROF_1)ZDEMI(J)))}$$

$$LRAC_2(J) = \frac{LVOPT}{(1 + \exp(-S \times (PROF_2)ZDEMI(J)))}$$

$$CUMULRACZ(J) = \sum LRAC_1(J) \times EPAIS1 CUMULRACZ(J) = \sum LRAC_2(J) \times EPAIS_2$$

$$TETSTOMATE(J) = \frac{1}{40} \ln(\frac{EOP(J)}{(2CUMULRACZ(J) \times PSISTO \times 10^-3)}) \times \ln(\frac{\frac{1}{rayon} \times ((ZRAC(J)))}{CUMULRACZ(J)})$$

$$TETA(J) = \begin{cases} \max[HUR1(J) - HUMIN(J), 0] \\ \frac{(TETA_1(J)+TETA_2(J))}{(ZRAC(J)\times 10)} \end{cases}$$

$$\begin{cases} \text{if} \quad ZRAC(J) \quad \leq \quad EPAIS1 \\ \text{else} \end{cases}$$

with

$$TETA_1(J) = \max[(HUR1(J) - HUMIN_1) \times EPAIS1, 0]$$

and

$$TETA_2(J) = \max[(HUR2(J) - HUMIN_2) \times EPAIS_2, 0]$$

$$EP(J) = \begin{cases} EOP(J) \\ \frac{(EOP(J)\times TETA(J))}{TETSTOMATE(J)} \end{cases}$$

$$\begin{cases} \text{if} \quad TETA(J) \quad > \quad TETSTOMATE(J) \\ \text{else} \end{cases}$$

$$EP_1(J) = \frac{(EP(J) \times ZRACZ((J))) \times EPAIS1}{CUMULRACZ(J)} EP_2(J) = \frac{(EP(J) \times ZRACZ((J))) \times EPAIS_2}{CUMULRACZ(J)}$$

$$EP_1(J) = \min((HUR1(J) - HUMIN_1) \times EPAIS1, EP_1(J)) EP_2(J) = \min((HUR2(J) - HUMIN_2) \times EPAIS2, EP(J) - EP_1(J))$$

$$HUR1(J) = (HUR1(J) - EP_1(J)) \times EPAIS1$$

$$HUR2(J) = (HUR2(J) - EP_2(J)) \times EPAIS_2$$

Water Budget

$$HUR1(J) = \frac{HUR1(J) \times EPAIS1 + PLUIE - DRAIN_1(J)}{EPAIS1}$$

with

$$DRAIN_1(J) = \begin{cases} HUR1(J) \times EPAIS1 + PLUIE - HUCC_1 \times EPAIS1 \\ 0 \end{cases}$$

$$\begin{cases} \text{if} \quad HUR1(J) EPAIS1 + PLUIE \quad > \quad HUCC_1 \times EPAIS1 \\ \text{else} \end{cases}$$

$$HUR2(J) = \frac{HUR2(J) \times EPAIS_2 + PLUIE - DRAIN_2(J)}{EPAIS_2}$$

$$DRAIN_2(J) = \begin{cases} HUR2(J) - EPAIS_2 + PLUIE - HUCC_2 \times EPAIS_2 \\ 0 \end{cases}$$

$$\begin{cases} \text{if} \quad HUR2(J) - EPAIS_2 + PLUIE \quad > \quad HUCC_2 \times EPAIS_2 \\ \text{else} \end{cases}$$

Stress Index

$$TETURG(J) = \frac{1}{40} \ln\left(\frac{EOP(J)}{(2CUMULRACZ(J) \times PSISTURG \times 10^-3)}\right) \times \ln\left(\frac{\frac{1}{rayon} \times ((ZRAC(J)))}{CUMULRACZ(J)}\right)$$

$$TURFAC(J) = \begin{cases} 1 \\ \frac{TETA(J)}{TETURG(J)} \end{cases}$$

$$\begin{cases} \text{if} \quad TETA(J) \quad > \quad TETURG(J) \\ \text{else} \end{cases}$$

References

[1] Aidala, V.: Parameter estimation via the Kalman filter, IEEE Trans. on Automatic Control, 22, 471–472, 1977.

[2] Andrews, B., Yi, T., and Iglesias, P.: Optimal noise filtering in the chemotactic response of Escherichia coli, PLoS computational biology, 2, e154, 2006.

[3] Arulampalam, M., Maskell, S., Gordon, N., and Clapp, T.: A tutorial on particle filters for online nonlinear/non-Gaussian Bayesian tracking, Signal Processing, IEEE Transactions on, 50, 174–188, 2002.

[4] Balaji, B. and Friston, K.: Bayesian state estimation using generalized coordinates, Proc. SPIE 8050, 2011.

[5] BARET, F.: CONTRIBUTION AU SUIVI RADIOMETRIQUE DE CULTURES DE CEREALES, Ph.D. thesis, 1986.

[6] Barndorff-Nielsen, O.: Exponentially Decreasing Distributions for the logarithm of Particle Size, in: Proc. Roy. Soc., vol. 353, pp. 401–419, London, 1977.

[7] Basso, B. and Ritchie, J.: Impact of compost, manure and inorganic fertilizer on nitrate leaching and yield for a 6-year maize-alfalfa rotation in Michigan, Agriculture, ecosystems & environment, 108, 329–341, 2005.

[8] Beal, M.: Variational Algorithms for Approximate Bayesian Inference, Ph.D. thesis, Gatsby Computational Neuroscience Unit, University College London, 2003.

[9] Brisson, N., Mary, B., Ripoche, D., Jeuffroy, M., Ruget, F., Nicoullaud, B., Gate, P., Devienne-Barret, F., Antonioletti, R., Durr, C., et al.: STICS: a generic model for the simulation of crops and their water and nitrogen balances. I. Theory, and parameterization applied to wheat and corn, Agronomie, 18, 311–346, 1998.

[10] Chen, G., Xie, Q., and Shieh, L.: Fuzzy Kalman filtering, Journal of Information Science, 109, 197–209, 1998.

[11] Corduneanu, A. and Bishop, C.: Variational Bayesian Model Selection for Mixture Distribution, in: Artificial Intelligence and Statistics, 2001.

[12] Diepen, C., Wolf, J., Keulen, H., and Rappoldt, C.: WOFOST: a simulation model of crop production, Soil use and management, 5, 16–24, 1989.

[13] Doucet, A. and Johansen, A.: A tutorial on particle filtering and smoothing: Fifteen years later, Handbook of Nonlinear Filtering, pp. 656–704, 2009.

[14] Doucet, A. and Tadić, V.: Parameter estimation in general state-space models using particle methods, Annals of the institute of Statistical Mathematics, 55, 409–422, 2003.

[15] Grewal, M. and Andrews, A.: Kalman Filtering: Theory and Practice using MATLAB, John Wiley and Sons, 2008.

[16] Gustafsson, F., Gunnarsson, F., Bergman, N., Forssell, U., Jansson, J., Karlsson, R., and Nordlund, P.: Particle filters for positioning, navigation, and tracking, Signal Processing, IEEE Transactions on, 50, 425–437, 2002.

[17] Hansen, S., Jensen, H., Nielsen, N., and Svendsen, H.: NPo-research, A10: DAISY: Soil Plant Atmosphere System Model, Miljøstyrelsen, 1990.

[18] Julier, S. and Uhlmann, J.: New extension of the Kalman filter to nonlinear systems, Proceedings of SPIE, 3, 182–193, 1997.

[19] Kalman, R. E.: A new approach to linear filtering and prediction problem, Trans. ASME, Ser. D, J. Basic Eng., 82, 34–45, 1960.

[20] Kim, Y., Sul, S., and Park, M.: Speed sensorless vector control of induction motor using extended Kalman filter, IEEE Trans. on Industrial Applications, 30, 1225–1233, 1994.

[21] Kotecha, J. and Djuric, P.: Gaussian particle filtering, IEEE Trans. on Signal Processing, 51, 2592–2601, 2003.

[22] Lee, J. and Ricker, N.: Extended Kalman filter based nonlinear model predictive control, Industrial & engineering chemistry research, 33, 1530–1541, 1994.

[23] Liu, J. and Chen, R.: Sequential Monte Carlo methods for dynamic systems, Journal of the American statistical association, pp. 1032–1044, 1998.

[24] Ljung, L.: Asymptotic behavior of the extended Kalman filter as a parameter estimator for linear systems, IEEE Trans. on Automatic Control, 24, 36–50, 1979.

[25] Mansouri, M., Snoussi, H., and Richard, C.: A nonlinear estimation for target tracking in wireless sensor networks using quantized variational filtering, Proc. 3rd International Conference on Signals, Circuits and Systems, pp. 1–4, 2009.

[26] Matthies, L., Kanade, T., and Szeliski, R.: Kalman filter-based algorithms for estimating depth from image sequences, International Journal of Computer Vision, 3, 209–238, 1989.

[27] Merwe, R. V. D. and Wan, E.: The square-root unscented Kalman filter for state and parameter-estimation, IEEE International Conference on Acoustics, Speech, and Signal Processing, 6, 3461–3464, 2001.

[28] Nounou, H. and Nounou, M.: Multiscale fuzzy Kalman filtering, Engineering Applications of Artificial Intelligence, 19, 439–450, 2006.

[29] Poyiadjis, G., Doucet, A., and Singh, S.: Maximum likelihood parameter estimation in general state-space models using

particle methods, in: Proc of the American Stat. Assoc, 2005.

[30] Sarkka, S.: On unscented kalman filtering for state estimation of continuous-time nonlinear systems, IEEE Trans. Automatic Control, 52, 1631–1641, 2007.

[31] Simon, D.: Kalman filtering of fuzzy discrete time dynamic systems, Applied Soft Computing, 3, 191–207, 2003.

[32] Simon, D.: Optimal State Estimation: Kalman, H_∞, and Nonlinear Approaches, John Wiley and Sons, 2006.

[33] Storvik, G.: Particle filters for state-space models with the presence of unknown static parameters, IEEE Trans. on Signal Processing, 50, 281–289, 2002.

[34] Tremblay, M. and Wallach, D.: Comparison of parameter estimation methods for crop models, Agronomie, 24, 351–365, 2004.

[35] Vermaak, J., Lawrence, N., and Perez, P.: Variational Inference for visual tracking, in: Conf. Computer Vision and Pattern Recognition, 2003.

[36] Wan, E. and Merwe, R. V. D.: The unscented Kalman filter for nonlinear estimation, Adaptive Systems for Signal Processing, Communications, and Control Symposium, pp. 153–158, 2000.

[37] Williams, J., Jones, C., Kiniry, J., and Spanel, D.: The EPIC crop growth model, Trans. ASAE, 32, 497–511, 1989.

[38] Yang, N., Tian, W., Jin, Z., and Zhang, C.: Particle filter for sensor fusion in a land vehicle navigation system, Measurement science and technology, 16, 677, 2005.

[39] Zhang, Z.: Parameter estimation techniques: A tutorial with application to conic fitting, Image and vision Computing, 15, 59–76, 1997.

Table 1: LSM model parameters and physical properties

Name	Meaning	True value
$ADENS$	Parameter of compensation between stem number and plant density	-0.8
$BDENS(plants.m^{-2})$	Maximum density above which there is competition between plants	1.25
$CROIRAC(cm.degree - day^{-1})$	Growth rate of the root front	0.25
$DLAIMAX(m^2.l.s.m^{-2}.degreedays^{-1})$	Maximum rate of the setting up of LAI	0.0078
$EXTIN$	Extinction coefficient of photosynthetic active radiation in the canopy	0.9
$KMAX$	Maximum crop coefficient for water requirements	1.2
$LVOPT(cm.root.cm^{-3}.s)$	Optimum root density	0.5
$PSISTO(bars)$	Absolute value of the potential of stomatal closing	10
$PSISTURG(bars)$	Absolute value of the potential of the beginning of decrease in the cellular extension	4
$RAYON(cm)$	Average radius of roots	0.02
$TCMIN(^\circ C)$	Minimum temperature of growth	6
$TCOPT(^\circ C)$	Optimum temperature of growth	32
$TURFAC$	turgescence stress index	–
$ZPENTE(cm)$	Depth where the root density is 1/2 of the surface root density for the reference profile	120
$ZPRLIM(cm)$	Maximum depth of the root profile for the reference profile	150
$HUMIN$	Minimum volumetric water content	$U(1.2, 1.7)$
$HUCC$	Usable reserve	$U(1.2, 1.7)$
$DENSITE(plm^2)$	Sowing density	$U(5, 7)$

Table 2: Root mean square errors (RMSE) of estimated states for EKF, PF and VF; 2008-2009

Technique	LAI	$HUR1$	$HUR2$
EKF	0.0634	0.0598	0.0297
PF	0.0358	0.0347	0.0251
VF	0.0190	0.0187	0.0122

Table 3: Root mean square errors (RMSE) of estimated states and mean of estimated parameter - case 1; 2008-2009

	RMSE			Mean at steady state
Technique	LAI	$HUR1$	$HUR2$	$ADENS$
EKF	0.0649	0.0602	0.0303	-0.8
PF	0.0364	0.0376	0.0257	-0.8
VF	0.0198	0.0190	0.0126	-0.8

Table 4: Root mean square errors of estimated states and mean of estimated parameters - case 2; 2008-2009

	RMSE			Means at steady state	
Technique	LAI	$HUR1$	$HUR2$	$ADENS$	$DLAIMAX$
EKF	0.1228	0.1244	0.0631	-0.8	did not converge
PF	0.0789	0.0808	0.0532	-0.8	0.0078
VF	0.0377	0.0389	0.0244	-0.8	0.0078

Table 5: Root mean square errors (RMSE) of estimated states and mean of estimated parameters - case 3; 2008-2009

	RMSE			Mean at steady state		
Technique	LAI	$HUR1$	$HUR1$	$ADENS$	$DLAIMAX$	$PSISTURG$
EKF	0.1794	0.1754	0.0957	-0.8	did not converge	did not converge
PF	0.1146	0.1186	0.0774	-0.8	0.0078	did not converge
VF	0.0608	0.0586	0.0369	-0.8	0.0078	4

Table 6: Root mean square errors (RMSE) of estimated states and mean of estimated parameter - case 1; 2009-2010

	RMSE			Mean at steady state
Technique	LAI	$HUR1$	$HUR2$	$ADENS$
EKF	0.0939	0.0901	0.0461	-0.8
PF	0.0542	0.0531	0.0342	-0.8
VF	0.0341	0.0357	0.0232	-0.8

Table 7: Root mean square errors of estimated states and mean of estimated parameters - case 2; 2009-2010

	RMSE			Means at steady state	
Technique	LAI	$HUR1$	$HUR2$	$ADENS$	$DLAIMAX$
EKF	0.1502	0.1589	0.0723	-0.8	did not converge
PF	0.0988	0.0957	0.0592	-0.8	0.0078
VF	0.0638	0.0557	0.0364	-0.8	0.0078

Table 8: Root mean square errors (RMSE) of estimated states and mean of estimated parameters - case 3; 2009-2010

	RMSE			Mean at steady state		
Technique	LAI	$HUR1$	$HUR1$	$ADENS$	$DLAIMAX$	$PSISTURG$
EKF	0.2143	0.2045	0.1061	-0.8	did not converge	did not converge
PF	0.1431	0.1433	0.0945	-0.8	0.0078	did not converge
VF	0.0847	0.0859	0.0594	-0.8	0.0078	4

Figure 1: Simulated LSM data used in estimation: state variables (leaf-area index LAI, volumetric water content of the layer 1;$HUR1$ and volumetric water content of the layer 2; $HUR2$).

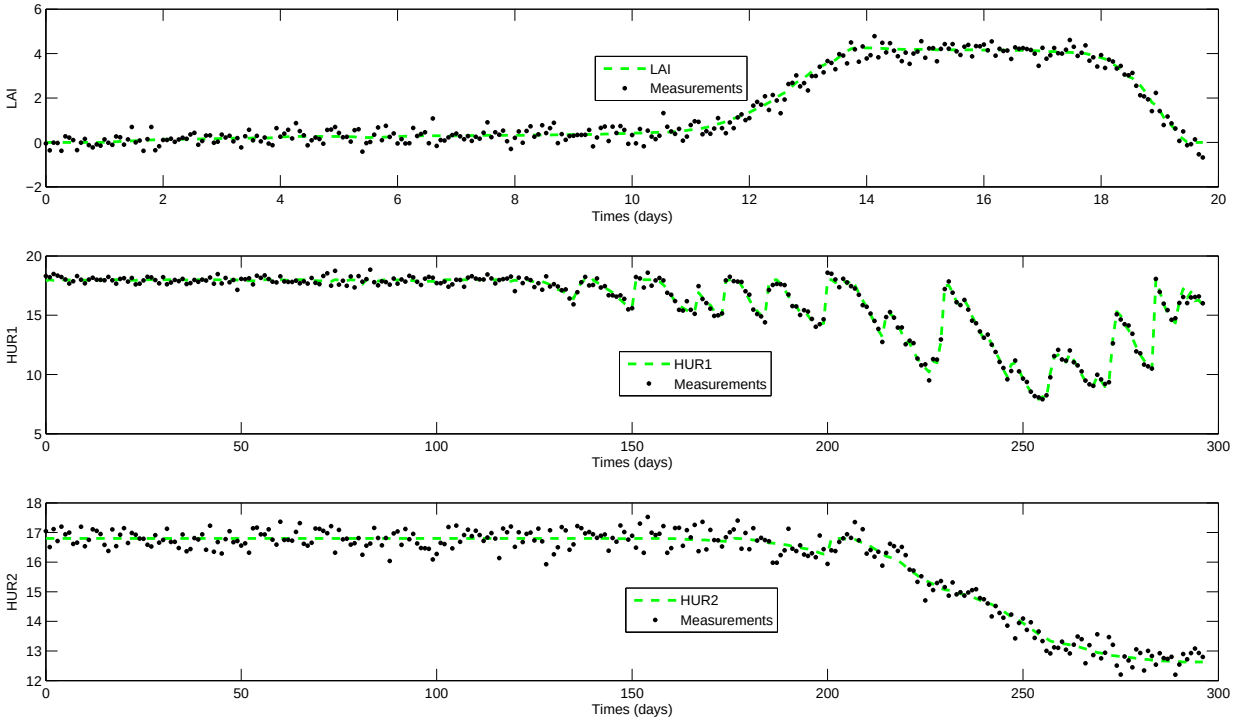

Table 9: Estimations of the three states versus noisy measurement variances.

	LAI	$HUR1$	$HUR1$
Technique	$\sigma_v^2 = 0.1$		
EKF	0.0634	0.0598	0.0297
PF	0.0358	0.0347	0.0251
VF	0.0190	0.0187	0.0122
	$\sigma_v^2 = 0.15$		
EKF	0.0636	0.0599	0.0299
PF	0.0367	0.0348	0.0253
VF	0.0192	0.0189	0.0124
	$\sigma_v^2 = 0.2$		
EKF	0.0639	0.0607	0.0305
PF	0.0369	0.0357	0.0259
VF	0.0196	0.0193	0.0128
	$\sigma_v^2 = 0.25$		
EKF	0.0641	0.0614	0.0315
PF	0.0383	0.0383	0.0276
VF	0.0201	0.0213	0.0152
	$\sigma_v^2 = 0.3$		
EKF	0.0671	0.0625	0.0328
PF	0.0395	0.0394	0.0283
VF	0.0214	0.0215	0.0163

Figure 2: Estimation of state variables using various state estimation techniques (comparative study 1).

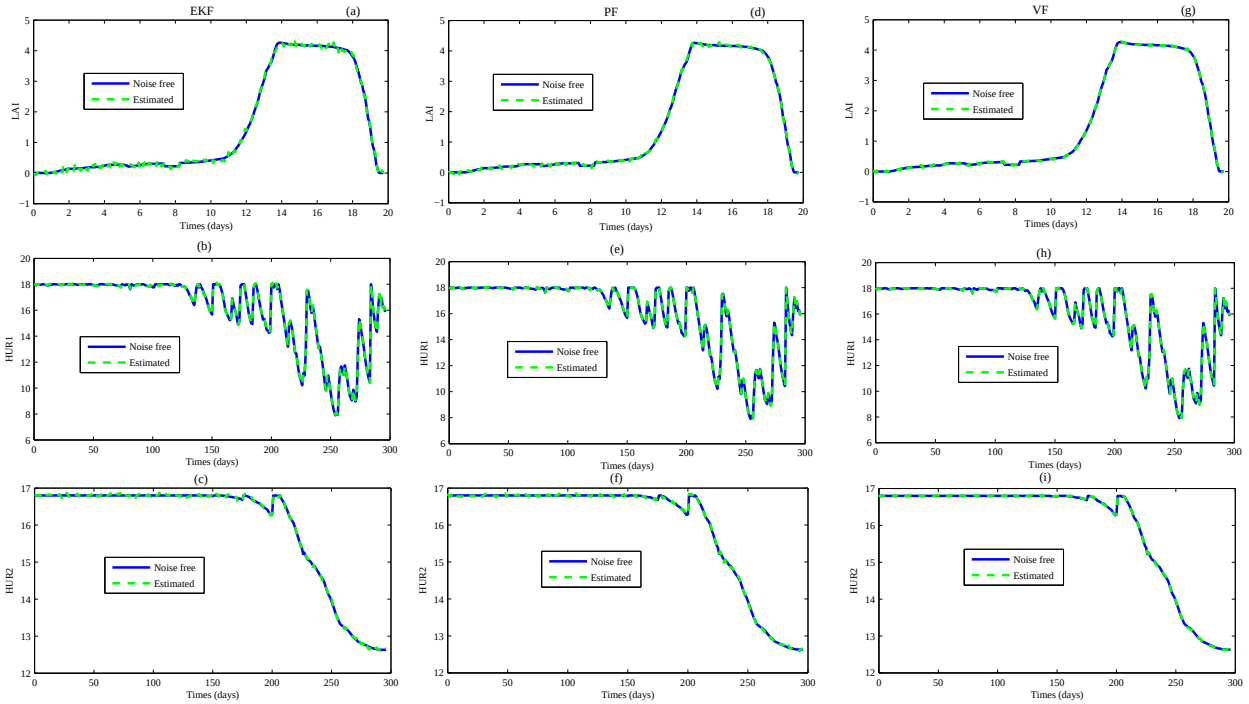

Figure 3: Estimation of $z = [LAI\ HUR1\ HUR2\ ADENS]^T$ using EKF - Case 1.

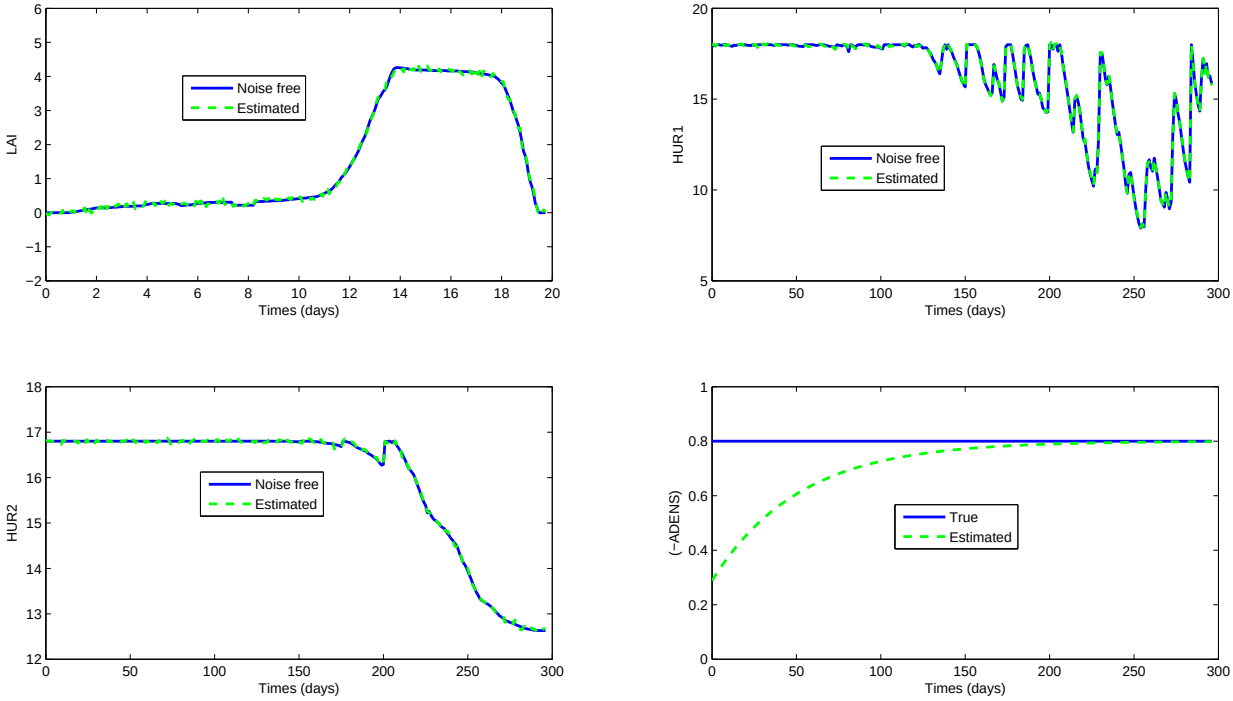

Figure 4: Estimation of $z = [LAI\ HUR1\ HUR2\ ADENS\ DLAIMAX]^T$ using EKF - Case 2.

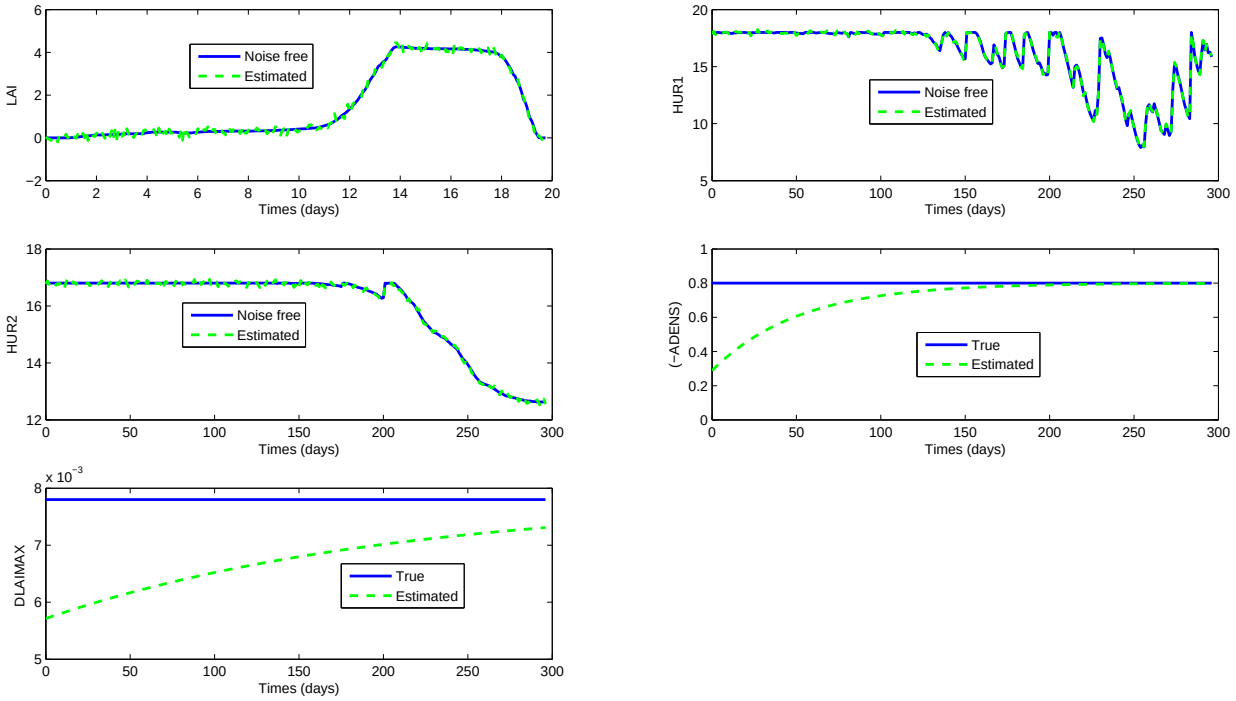

Figure 5: Estimation of $z = [LAI\ HUR1\ HUR2\ ADENS\ DLAIMAX\ PSISTURG]^T$ using EKF - Case 3.

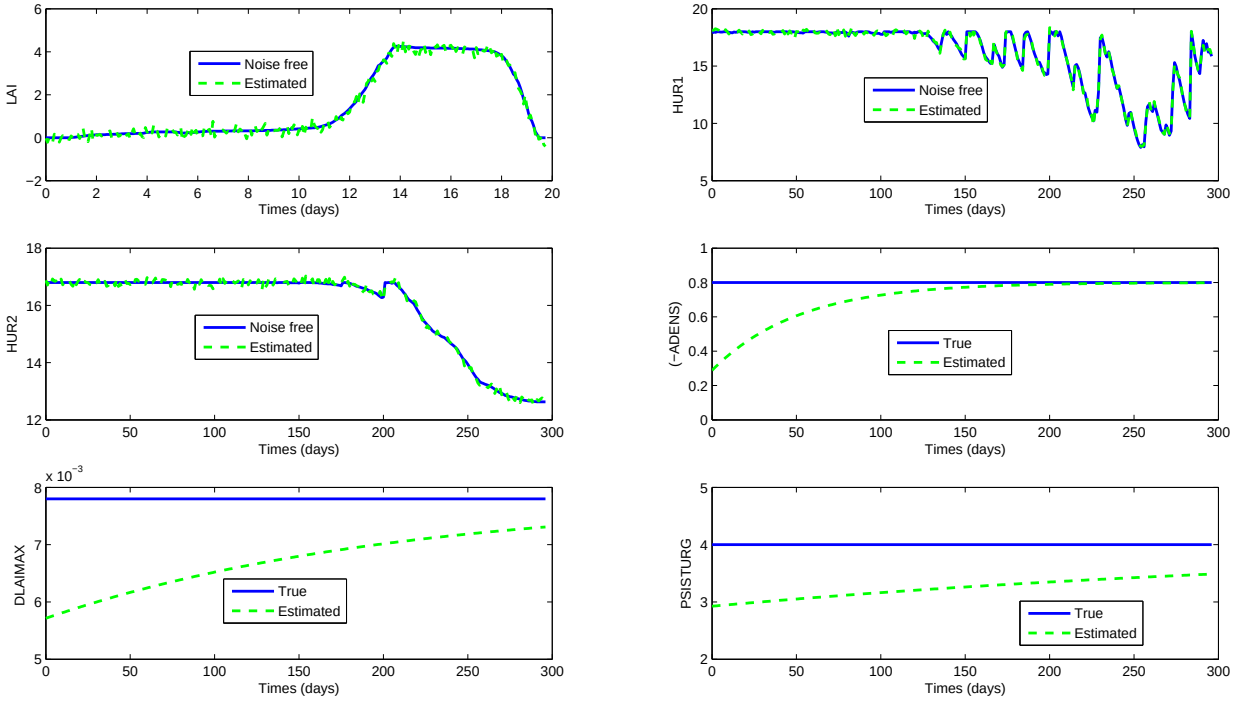

Figure 6: Estimation of $z = [LAI\ HUR1\ HUR2\ ADENS]^T$ using PF - Case 1.

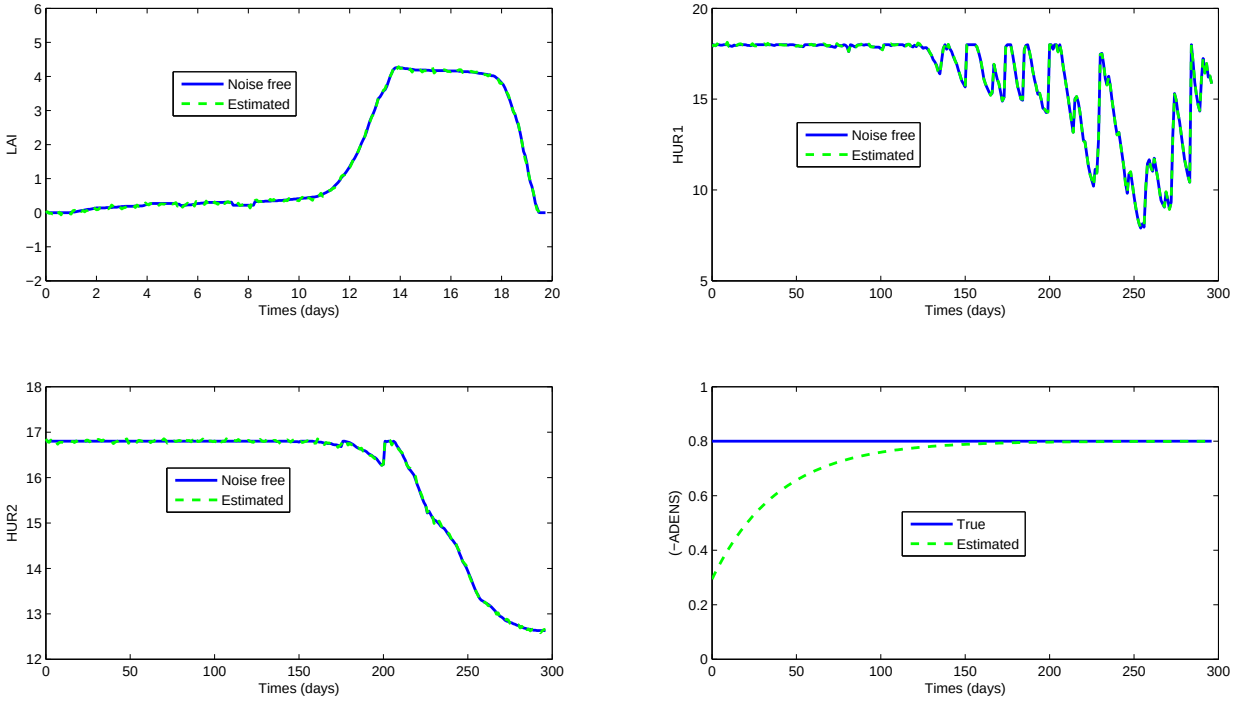

Figure 7: Estimation of $z = [LAI\ HUR1\ HUR2\ ADENS\ DLAIMAX]^T$ using PF - Case 2.

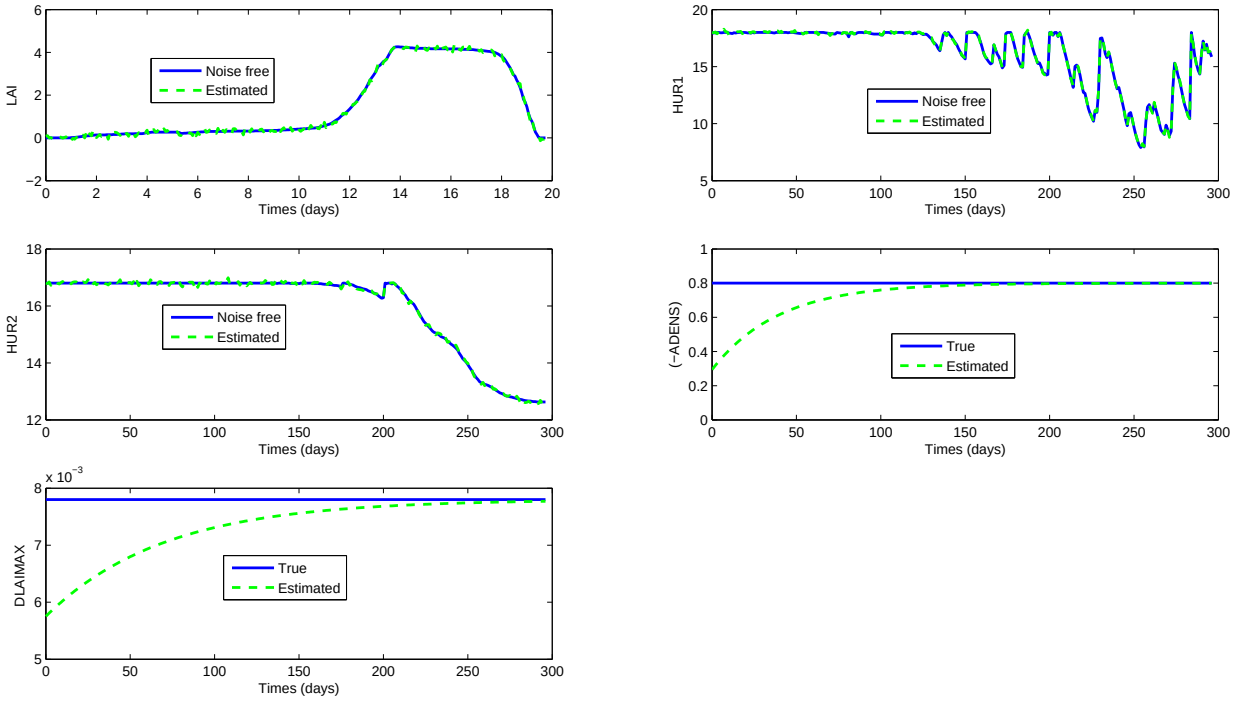

Figure 8: Estimation of $z = [LAI\ HUR1\ HUR2\ ADENS\ DLAIMAX\ PSISTURG]^T$ using PF - Case 3.

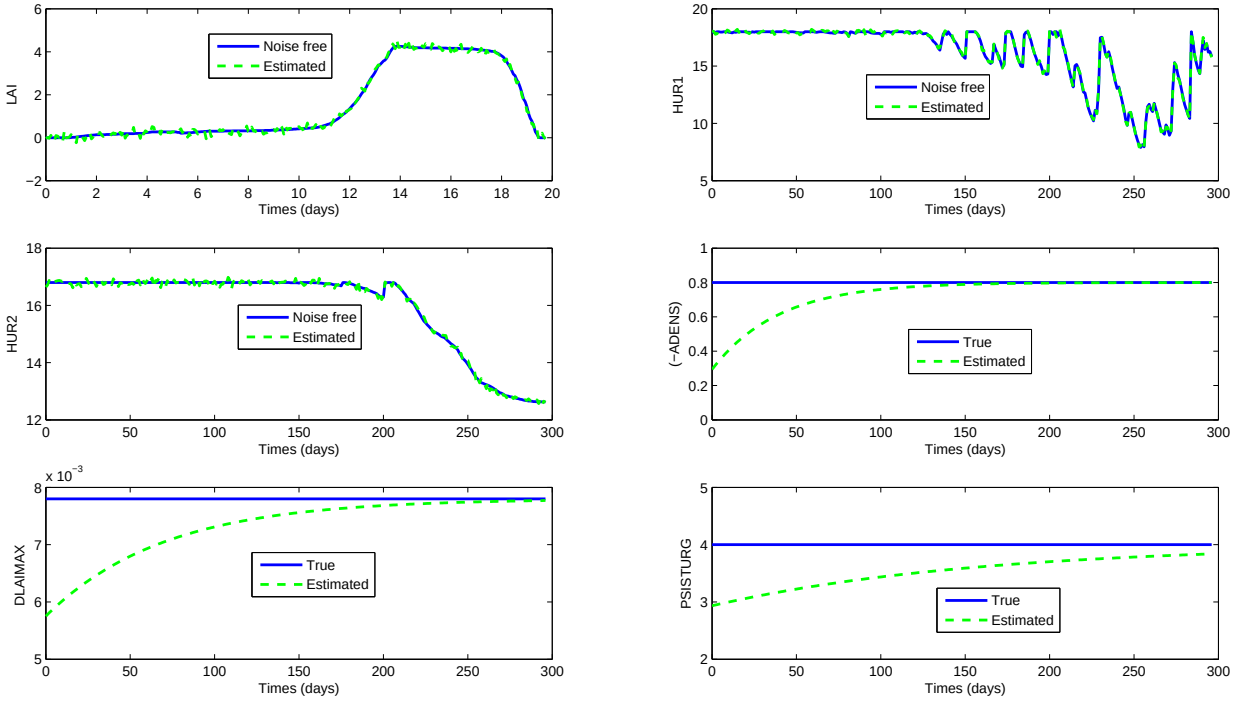

Figure 9: Estimation of $z = [LAI\ HUR1\ HUR2\ ADENS]^T$ using VF - Case 1.

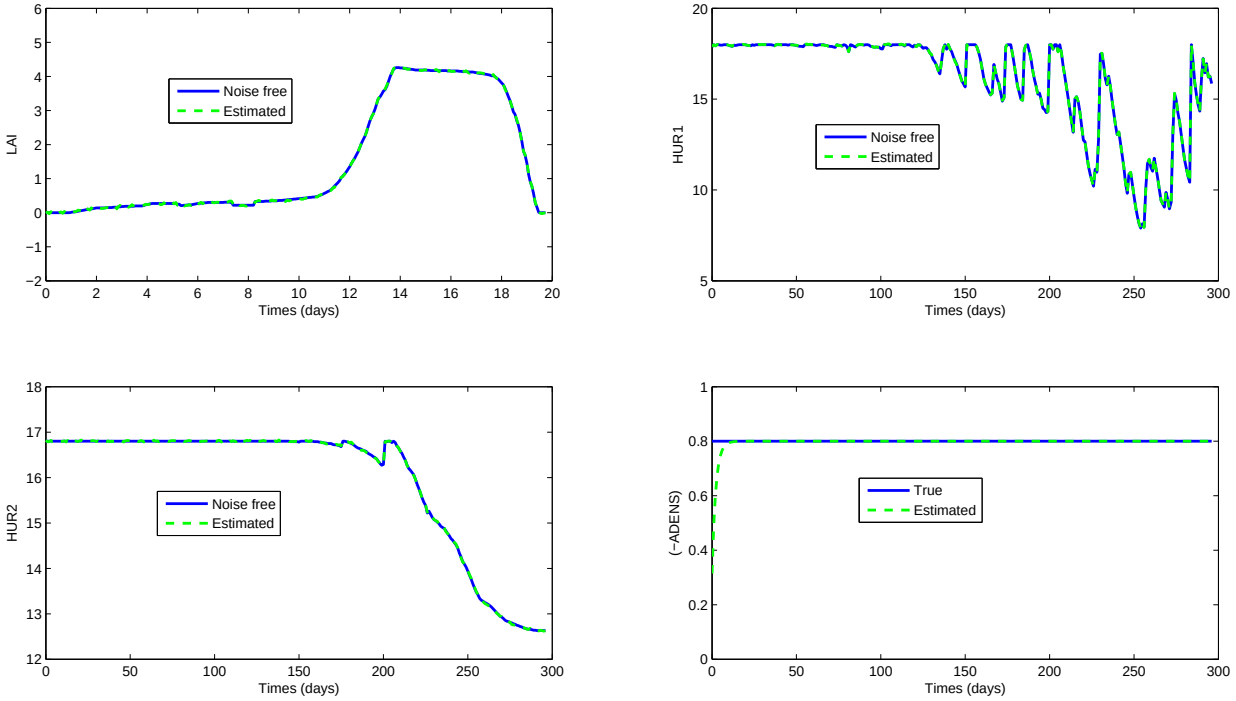

Figure 10: Estimation of $z = [LAI\ HUR1\ HUR2\ ADENS\ DLAIMAX]^T$ using VF - Case 2.

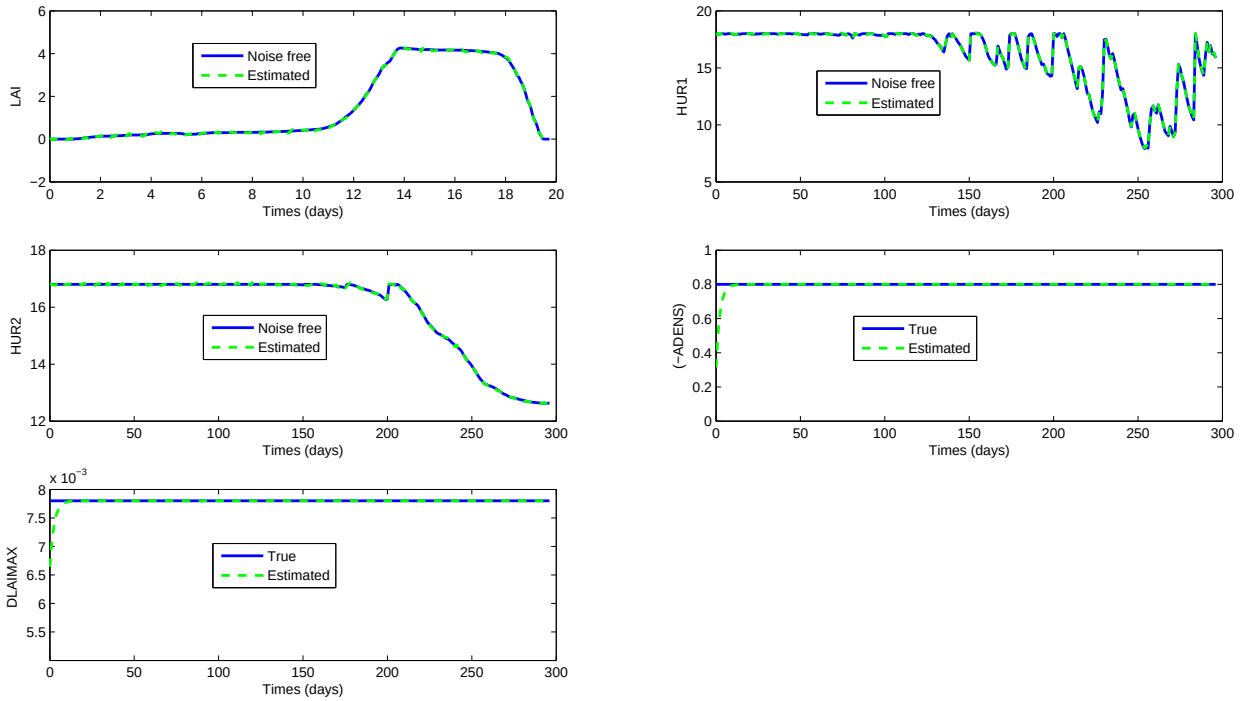

Figure 11: Estimation of $z = [LAI\ HUR1\ HUR2\ ADENS\ DLAIMAX\ PSISTURG]^T$ using VF - Case 3.